

Consistencies and inconsistencies in redshift-independent distances

José Antonio Nájera^{1*} and Harry Desmond^{1†}

¹*Institute of Cosmology & Gravitation, University of Portsmouth, Dennis Sciama Building, Portsmouth, PO1 3FX, UK*

19 March 2025

ABSTRACT

Redshift-independent distances underpin much of astrophysics, and there exists a plethora of methods to estimate them. However, the extent to which the distances they imply are consistent, while crucial for the integrity of the distance ladder, has been little explored. We construct a statistical framework to assess both internal (between measurements with the same method) and external (between-method) consistency by comparing differences between distances to their quoted statistical uncertainties in the NASA/IPAC Extragalactic Database of Distances (NED-D). 66 of the 76 indicators in NED-D are amenable to a consistency test by having at least two measurements to the same galaxy or at least one measurement to a galaxy also measured by another method. We find that only 12 of these methods produce self-consistent distances across literature determinations, of which 7 are also consistent with distances to the same galaxies measured by all other methods. The most consistent 6 methods (M-stars luminosity, Novae, Masers, Globular Cluster Fundamental Plane, O- and B-type Supergiants and BL Lac Luminosity) also give similar average distances to the mean of all indicators, while the 7th (Proper Motion) underestimates distances relative to the mean by 17.1%. We also investigate consistency of Cepheid distances in the SH0ES 2022 catalogue, finding no evidence for unaccounted-for systematics. Our NED-D results imply that considerable work remains to obtain reliable distances by a multitude of methods, a crucial endeavour for constructing a multiply cross-checked and fully robust distance ladder.

Key words: galaxies: distances and redshifts – cosmology: distance scale – methods: statistical – astronomical data bases

1 INTRODUCTION

Much of modern cosmology depends on redshift-independent distances to astrophysical objects. Historically the first application of such distances was to combine with redshifts to produce a “Hubble diagram”, which provided the first evidence that the Universe is expanding (Hubble 1929) and that the expansion of the Universe is accelerating (Riess et al. 1998; Perlmutter et al. 1999). Hubble diagrams remain a crucial tool in cosmology today, providing precise constraints on parameter values and distinguishing between different gravitational and cosmological models (e.g. Li et al. 2021; Pourjaghi et al. 2022; Rezaei et al. 2022; Anton & Clifton 2024). This is particularly pertinent currently in the context of the “Hubble tension”, a claimed $\sim 5\sigma$ tension (Riess et al. 2022) between the present-day expansion rate of the Universe, H_0 , derived from the Hubble diagram versus inferred from the Cosmic Microwave Background (CMB) assuming the expansion history of the Universe implied by the standard model

of cosmology, Λ CDM (for recent reviews see Freedman & Madore 2023; Riess & Breuval 2024). Even more recently, the Hubble diagrams of baryon acoustic oscillations and Type Ia supernovae (SNIa) appear to favour dynamical dark energy models over a cosmological constant for explaining the Universe’s accelerated expansion (DESI Collaboration et al. 2024).

Assuming a cosmological model (e.g. Λ CDM) with calibrated values for its free parameters, distances in the Universe may be estimated from objects’ redshifts alone. However, within the local ~ 100 Mpc redshifts provide inaccurate distance estimates because galaxies’ velocities are not predominantly due to the expansion of the Universe. There is a significant contribution from “peculiar velocities”, galaxies’ individual motions superimposed on the Hubble flow generated by gravitational interaction with their cosmic environment (for reviews see Strauss & Willick 1995; Turner 2024). If distances to such galaxies can be measured redshift-independently then peculiar and expansion velocities can be determined separately. The pattern of peculiar velocities provides evidence concerning the large-scale structure of the local Universe (Dupuy & Courtois 2023; Valade et al. 2024),

* E-mail: antonio.najera@port.ac.uk

† E-mail: harry.desmond@port.ac.uk

the growth rate of cosmic structure (Boruah et al. 2020; Said et al. 2020; Stiskalek et al. 2025), extensions to General Relativity (Lyall et al. 2023, 2024), the large-scale isotropy of the Universe (e.g. Feindt et al. 2013; Watkins et al. 2023) and the typicality or otherwise of the Milky Way’s place in the Universe (Bovy et al. 2009; McMillan 2016).

Given these many and varied opportunities, much effort has naturally been devoted to measuring redshift-independent (or direct) distances. This is done in a series of steps, likened to rungs of a ladder: direct geometric methods (mainly parallax) are used to establish distances to nearby objects (mainly stars within the Milky Way), which are in turn used to calibrate objects on the “first rung” of the distance ladder. The most common such objects are Cepheid stars—which obey a linear relation between their distance-independent pulsation period and distance-dependent luminosity (for reviews see Freedman & Madore 2024; Anderson 2024)—and the Tip-of-the-Red-Giant-Branch (TRGB) feature of the colour–magnitude diagram, which has a fixed luminosity arising from the Helium flash in an electron-degenerate stellar core of intermediate-to-low-mass stars. Hence, it acts as a standard candle (Lee et al. 1993; for a review see Li & Beaton 2024). Once calibrated, these methods can be used to establish direct distances to ~ 50 Mpc. They in turn are used to calibrate the ladder’s “second rung”. A key method here is SNIa which are standardisable candles: after correction for the colour and width of their light-curves they have a fixed luminosity, so that if this is calibrated using e.g. Cepheids or TRGB the measured flux determines the distance. This allows the Hubble diagram to be extended out to $z \approx 1$ (~ 3 Gpc; Brout et al. 2022; Rubin et al. 2023; Vincenzi et al. 2024).

Parallax–Cepheid/TRGB–SNIa is the best-known route to the distance ladder, but there is in fact a plethora of methods for determining redshift-independent distances. Based on standard candle, standard ruler, standard siren and other techniques, these employ different objects, different physics, different measurement methods and different systematics, and operate at various locations of the ladder (i.e. requiring varying degrees of calibration). Given the crucial importance of the distance ladder for cosmology, and the tensions it has thrown up, it seems prudent to compare carefully as wide as possible a range of methods to assess possible systematic errors and with an eye to swapping out or supplementing some methods for others in constructing a maximally robust, precise and far-reaching ladder.

That is the aim of this paper. We take as our starting point the *NASA/IPAC Extragalactic Database of Distances* (NED-D),¹ a compilation containing $>270,000$ extragalactic distances measured to $>140,000$ galaxies using 76 different distance indicators (Steer et al. 2016). Our particular focus here is on quantifying the statistical consistency of distances measured to the same galaxies, either of multiple estimates with the same method (self-consistency) or between methods (cross-consistency). This depends crucially on the quoted uncertainties, which are themselves model-dependent quantities with their own uncertainties. We apply the same methods to the Supernova H_0 for the Equation of State (SH0ES) pipeline as a leading example of distance ladder-based H_0 inference framework (Riess et al. 2009, 2011, 2012, 2022). Our

approach will allow us to determine which methods appear most reliable, and whether systematics may be biasing literature inferences employing the distance ladder. In case of inconsistency we can establish whether this is due to under- or over-estimated uncertainties and/or mean shifts in all distances inferred by some method. This provides a stepping stone towards construction of a more confidently reliable ladder employing multiple redshift-independent distance methods.

Our work builds on that of Singh (2021), who identified a systematic underestimation in uncertainties in NED-D that is most prominent for the most widespread methods and growing over time. This suggests that the precision of e.g. H_0 inferred from the distance ladder may be overstated, clearly of great importance to the aforementioned tension. Our improvements on this analysis are first to improve the statistical measure and test of consistency and second to perform an independent analysis of the SH0ES 2022 results (Riess et al. 2022) as the first catalogue claiming a 5σ Hubble tension. This provides information on whether inconsistencies in distance measurements may be responsible for (some of) the tension.

The structure of the paper is as follows. In Sec. 2 we describe the NED-D and SH0ES data that we analyse. Sec. 3 details our statistical methodology, while Sec. 4 presents our findings. We discuss more general ramifications of the work as well as caveats in Sec. 5, and conclude in Sec. 6.

2 OBSERVATIONAL DATA

2.1 NED-D

NED-D is an online compilation of redshift-independent extragalactic distances containing $> 270,000$ distance measurements to $> 140,000$ galaxies using 76 different methods (Steer et al. 2016). These methods, categorised as standard candles, standard rulers or “secondary” (defined as having a precision $\sim 20\%$ as opposed to the other “primary” methods with precision $\lesssim 10\%$; Steer et al. 2016), are as follows:

- **Standard candles:** AGN time lag, Asymptotic Giant Branch Stars (AGB), B-type Stars (B Stars), BL Lac Object Luminosity (BL Lac Luminosity), Black Hole, Blue Supergiant, Brightest Cluster Galaxy (BCG), Brightest Stars, Carbon Stars, Cepheids, Colour-Magnitude Diagrams (CMD), Delta Scuti, Flux-Weighted Gravity-Luminosity Relation (FGLR), Gamma-Ray Burst (GRB), Globular Cluster Luminosity Function (GCLF), Globular Cluster Surface Brightness Fluctuations (GC SBF), HII Luminosity Function (HII LF), Horizontal Branch, M Stars luminosity (M Stars), Miras, Novae, O- and B-type Supergiants (OB Stars), Planetary Nebula Luminosity Function (PNLF), Post-Asymptotic Giant Branch Stars (PAGB Stars), Quasar spectrum, RR Lyrae Stars, Red Clump, Red Supergiant Variables (RSV Stars), Red Variable Stars (RV Stars), S Doradus Stars, SNIa SDSS, SX Phoenixis Stars, Short Gamma-Ray Bursts (SGRB), Statistical, Subdwarf Fitting, Sunyaev-Zeldovich Effect (SZ effect), Surface Brightness Fluctuations (SBF), Tip of the Red Giant Branch (TRGB), Type II Cepheids, Type II Supernovae Radio (SNII radio), Type Ia Supernovae (SNIa), White Dwarfs, Wolf-Rayet, Gravitational Wave (Grav. Wave).

¹ <https://ned.ipac.caltech.edu/Library/Distances/>

- **Standard rulers:** CO ring diameter, Dwarf Galaxy Diameter, Eclipsing Binary, Globular Cluster Radii (GC radius), Grav. Stability Gas. Disk, Gravitational Lenses (G Lens), HII Region Diameters (HII), Jet Proper Motion, Masers, Orbital Mechanics (Orbital Mech.), Proper Motion, Ring Diameter, Type II Supernovae, Optical (SNII Optical).
- **Secondary methods:** D-Sigma, Diameter, Dwarf Ellipticals, Faber-Jackson, Fundamental Plane (FP), GC K vs. (J-K), GeV TeV ratio, Globular Cluster Fundamental Plane (GC FP), H I + optical distribution, Infra-Red Astronomical Satellite (IRAS), L(Hbeta)-sigma, LSB galaxies, Magnitude, Mass Model, Radio Brightness, Sosies, Tertiary, Tully Estimate (Tully est), Tully-Fisher.

More details on the physics of the methods can be found on the NED-D website.² Some measurements are quoted for a specific value of H_0 , in which case we rescale them to correspond to $H_0 = 70\text{km/s/Mpc}$. Others are quoted for a specific value of the distance modulus to the Large Magellanic Cloud (LMC), in which case we rescale them to $\mu_{\text{LMC}} = 18.50$.³ Other measurements come with neither an assumed H_0 nor an assumed μ_{LMC} , in which case we cannot standardise them. We discard measurements without a quoted uncertainty, which cannot be statistically analysed. We consider all measurements to be independent. Various measures of average distance over multiple indicators in NED-D were defined and compared in Steer (2020). We denote distance indicators in NED-D with `this font`.

2.2 SHOES 2022

We also consider the Cepheid catalogue used by the SHOES collaboration in 2022. This is the latest full release of the SHOES data. Furthermore, this is particularly pertinent as it has been used to argue for a $> 5\sigma$ Hubble tension (Riess et al. 2022).

The SHOES 2022 catalogue includes 3130 Cepheid measurements across 40 galaxies. Two of them correspond to first-rung galaxies with direct geometric distances, one non-SNIa host galaxy, with the remainder in the second rung used to calibrate SNIa. The third calibration galaxy, the Milky Way (MW), imposes an effective Gaussian prior on the Wesenheit absolute magnitude at a period of 10 days and solar metallicity $M_{H,1}^W$. The full catalogue is available in three FITS files. The data does not include the distance modulus μ to each Cepheid, but rather the period P , Wesenheit apparent magnitude m_H^W in the F160W passband and excess metallicity $[O/H]$ along with their covariance matrix. The absolute magnitude can be derived from the Period–Luminosity (PL) relation via (Riess et al. 2022)

$$\mu_0 = m_H^W - M_{H,1}^W - b_W(\log_{10} P - 1) - Z_W[O/H], \quad (1)$$

² <https://ned.ipac.caltech.edu/Library/Distances/distintro.html>

³ Within the set of methods calibrated against either H_0 or μ_{LMC} the choice of 70km/s/Mpc and 18.5 is simply a convention and changing it will not affect differences between the extragalactic distance moduli. However this choice does affect relative distances between methods calibrated with H_0 or μ_{LMC} . Thus H_0 not being 70 km/s/Mpc or μ_{LMC} not being 18.5 may contribute to some of the inconsistencies we uncover.

where $M_{H,1}^W$ is the fiducial Wesenheit absolute magnitude at $P = 10$ days and solar metallicity, and b_W and Z_W are parameters defining the empirical relation between these variables.

Riess et al. (2022) quote constraints for these parameters, which would enable us to compute the individual distance modulus for all Cepheids in the catalogue. However, it does not include the full covariance matrix necessary to derive their uncertainties. Thus, we ran a Monte Carlo Markov Chain (MCMC) analysis using the `emcee` sampler⁴ (Foreman-Mackey et al. 2013) with 100 walkers and > 50 times the auto-correlation length in samples to ensure convergence. The set of inferred parameters includes the distance modulus to 38 galaxies, the differences between the predicted and geometric distance moduli for the two first-rung galaxies (minimised to calibrate the PL relation), the PL relation parameters previously mentioned, the absolute magnitude of SNIa M_B^0 , Δz_p (a parameter accounting for possible systematics associated with ground-based observations), and $5 \log H_0$.

Following SHOES we use wide uniform priors in all parameters. The χ^2 function is provided in Eq. 6 in (Riess et al. 2022). The contribution from the MW Cepheids is entered as two external constraints in $M_{H,1}^W$ from the Hubble Space Telescope (HST) and Gaia EDR3. We do the inference by using the `emcee` code provided by Riess et al. (2022). By doing this, we get their same constraints, including $H_0 = 73.04 \pm 1.01\text{ km/s/Mpc}$. This produces a fit to the distance modulus of each galaxy as an average over the Cepheids they contain. This is accurate as long as the individual Cepheids are statistically consistent, which we study both for the catalogue as a whole and each galaxy separately. Finally, we get the covariance matrix for the parameters $\{M_{H,1}^W, b_W, Z_W\}$ over the chains, and used this result to derive the covariance matrix for the Cepheid distances using

$$\text{Cov}(\mu_{0k}, \mu_{0l}) = \sum_{i=1}^M \sum_{j=1}^M \left(\frac{\partial \mu_{0k}}{\partial \theta_i} \right) \left(\frac{\partial \mu_{0l}}{\partial \theta_j} \right) \text{Cov}(\theta_i, \theta_j), \quad (2)$$

where $\theta_{i,j}$ are the parameters $\{m_{H,(k,l)}^W, M_{H,1}^W, b_W, Z_W\}$ ($M = 4$). This ensures that the uncertainties are properly propagated into the distance moduli. With this result we can perform our consistency analysis on this catalogue. We carry this out on the whole catalogue and also on each galaxy separately to search for galaxy-specific systematics.

3 METHODOLOGY

3.1 Quantifying consistency

We perform two kinds of consistency tests: internal (or self) and external (or cross). For the internal test we consider the measurements for a given method and a given galaxy with each other, while for the external test we compare for each galaxy the measurements from every pair of methods. This naturally restricts us to galaxies for which there are multiple measurements.

We compute the difference between each pair of measurements using

$$\Delta_{ij} = \sqrt{(\mu_i - \mu_j)^T \Sigma_{ij}^{-1} (\mu_i - \mu_j)}, \quad (3)$$

⁴ <https://emcee.readthedocs.io/en/stable/>

where $\mu_{i,j}$ are the distance moduli, and Σ is the covariance between the two measurements. In this case Σ_{ij} is a number given by $\sigma_{\mu_i}^2 + \sigma_{\mu_j}^2 - 2 \text{Cov}(\mu_i, \mu_j)$ where $\sigma_{\mu_{i,j}}$ are the diagonal uncertainty terms and $\text{Cov}(\mu_i, \mu_j)$ the cross-term between the two measurements. Note that $\text{Cov}(\mu_i, \mu_j)$ is assumed to be zero for all NED-D measurements, and hence only plays a role in the SH0ES analysis. Eq. 3 gives the Mahalanobis distance (Mai-Jalanobis 1936) describing the difference in units of σ between the measurements. It would be distributed as a standard half-normal if μ_i and μ_j were scattered from a common true value by their uncertainties (positive part of the standard normal $\mathcal{N}(\mu = 0, \sigma^2 = 1)$ for $x \geq 0$).⁵

We calculate the following quantities:

- (i) For each method in the NED-D catalogue, we take all the galaxies having at least two measurements. We compute Δ_{ij} for all possible pairs across all galaxies in that method. This quantifies internal consistency.
- (ii) For all possible pairs of methods in the NED-D catalogue, we take all galaxies having at least one measurement by both methods. We compute Δ_{ij} for all possible pairs across all galaxies for this method pair. This quantifies external consistency.
- (iii) For the SH0ES 2022 catalogue, we compute Δ_{ij} for all possible measurement pairs across all galaxies. This is a global measure of consistency across the catalogue.
- (iv) For each galaxy individually in the SH0ES 2022 catalogue, we compute Δ_{ij} for all possible measurement pairs in this galaxy. This measures consistency for each galaxy separately.

This produces in each case a Δ_{ij} distribution, which we then compare to the expected standard half-normal distribution. If the Δ_{ij} could not plausibly have been drawn from this distribution this implies an inconsistency, which could be due to unaccounted-for systematic errors, underestimated or overestimated uncertainties, outliers, inconsistent normalisations of distance and/or other problems. To assess this consistency we compare the Δ_{ij} and standard half-normal distributions using the Kullback–Leibler divergence (KLD; Kullback & Leibler 1951; MacKay 2003).⁶ This is defined by

$$D_{KL}(P|Q) = \int_{-\infty}^{\infty} dx P(x) \log \left(\frac{P(x)}{Q(x)} \right), \quad (4)$$

where P is the empirical probability distribution function (pdf), Q is the comparison pdf (standard half-normal). We validated our results by computing the KL divergence using the Simpson’s rule and the entropy (given by

⁵ Eq. 3 may be compared to eq. 1 of Singh (2021), $\Delta_{12} = |\mu_1 - \mu_2|/\sigma_{\mu_1}$. This has the disadvantage of not being symmetric under $\mu_1 \leftrightarrow \mu_2$, and of comparing a random variable to a fixed number in its treatment of the uncertainties.

⁶ One might think first to use the Kolmogorov–Smirnov (KS) test (An 1933; Smirnov 1948). This is however unsuitable, as the p -value of a given test statistic depends on the size of the input array, here the number of measurement pairs. That this is not the number of independent measurements biases p low, which can lead one to infer inconsistency even for mock data drawn from a standard half-normal when the sample size is large. This can be addressed in the case of self-consistency by computing the p -value using the number of independent measurements rather than the number of pairs, but it is not possible to assign unambiguously a number of effective samples in the cross-consistency test.

$\sum_i P(x_i) \log(P(x_i)/Q(x_i))$) and found that they give consistent comparable results with each other. Eq. 4 measures the similarity of the two pdfs. To convert the discrete measurements into a continuous KL pdf we apply Gaussian Kernel Density Estimation (KDE; Virtanen et al. 2020) with a bandwidth of the form $h = Cn^{-1/5}$ where n is the number of measurement pairs. We then apply either Scott’s (Scott 2015) or Silverman’s (Silverman 2018) method for setting the bandwidth, which we find to give near-identical results. We also find similar results using a histogram (top-hat KDE) rather than Gaussian KDE.

This measures the “distance” between the measured distribution and standard half-normal, but does not by itself tell us how unexpected any such distance is. To determine this, we compute the KLD of 10,000 mock datasets generated assuming that the Δ_{ij} test statistic precisely follows a standard half-normal. This produces the KLD distribution corresponding to the null hypothesis that the measurements are perfectly consistent up to scatter described by their uncertainties. This allows us to compute a p -value for rejection of the null hypothesis as the fraction of mock datasets having a KLD greater than the empirical one. We use a threshold of 0.05 to reject the null hypothesis. If $p > 0.05$ there is insufficient evidence to conclude that the measurements are not simply scattered by their uncertainty distributions; we term this “consistency”. For the simulations to be on equal footing to the real data, we simulate the same number of measurement pairs as exists in NED-D. This ensures that the p -value is independent of the number of galaxies and measurements.

Note that defining the p -value as the fraction *greater* than the measured value corresponds to us doing a one-tailed hypothesis test, searching for inconsistency only in the direction that the real data is *less* like a standard normal than the mocks. It is in fact possible for the data to be abnormal in the other direction, viz. *more* like a standard normal than would be expected under the null hypothesis. This would be tested by a two-tailed test that calculates p as the fraction of mock datasets *more extreme* than the real data. We choose simply to flag such “anomalously good” cases, which correspond to the one-tailed p -value being > 0.975 .

3.2 Extracting insight from inconsistency

The result of Sec. 3.1 is a p -value for rejection of the null hypothesis of consistency between each method and any other (including itself) in the case of NED-D, and between all the Cepheid distances in the SH0ES catalogue either globally or galaxy-by-galaxy.

There are a number of insights we can draw from this. The first is to identify the “best” (most consistent) distance indicators in the NED-D catalogue. To achieve this, we order the methods in increasing external consistency fraction. For a given indicator, we consider all other indicators that share at least one galaxy. We define the external consistency fraction as the number of such pairs that are consistent divided by the total number. Then, we remove the method with the lowest percentage external consistency and again compute the external consistency percentage assuming that a discarded method is responsible for inconsistency in any pair containing it. We repeat this process until we remain with a set of methods that have complete external consistency with each other. This is the maximal set of externally consistent methods.

Next we can learn about the cause of the inconsistencies. To learn whether an inconsistency derives under- or overestimated uncertainties we perform an additional analysis by rescaling the distance uncertainties by the ratio of the uncertainty of each galaxy to the standard half-normal standard deviation ($\sigma'_i = (\Sigma/\sqrt{1-2/\pi})\sigma_i$ where σ'_i is the rescaled uncertainty of a given distance measurement, Σ is the standard deviation of the empirical pdf before the rescaling and σ_i is the original uncertainty). If this produces consistency, the original inconsistency must have been caused by the uncertainties. In that case, we then compare the variance of the Δ_{ij} distribution to that of the standard half-normal $(1-2/\pi)$. If it is higher, then the uncertainties are underestimated, and vice versa.

For the case of external consistency the situation is more complex as an inconsistency could derive from inconsistent means of the μ_i and μ_j distributions rather than anything to do with the uncertainties. To disentangle the possible causes, we repeat the consistency analysis with two modifications. First, for each galaxy in the method pair, we computed the mean distance modulus over the measurements of each method. We then shift the mean of one method onto that of the other and repeat the consistency test. If this transformation produces consistency, the original inconsistency must have been due to inconsistent means. The second modification is instead of shifting the means to rescale the uncertainties by the relative standard deviations of the μ distributions. If this produces consistency, the original inconsistency must have come from the uncertainties. Note that having inconsistent means and uncertainties are not mutually exclusive. It is possible for a given method pair to have both, in which case neither of the above modifications will produce consistency by itself, but combining both of them will yield an acceptable p -value. If even in this case the test returns inconsistency, this must be due to other effects such as outliers, non-Gaussian uncertainties or systematic errors. We call this an ‘‘essential inconsistency,’’ in the sense that it cannot (easily) be removed.

We are also interested in studying the tendency of each method to produce smaller or larger distances relative to the others. This will help to determine the methods that under- or overestimate distances with respect to other methods. For any given method pair and galaxy, we calculate the uncertainty-weighted mean distance modulus as

$$\bar{\mu}_g^i = \frac{\sum_k \mu_{g,k}^i / (\sigma_{g,k}^i)^2}{\sum_k 1 / (\sigma_{g,k}^i)^2} \quad (5)$$

and its uncertainty $\sigma_g^i = 1/\sqrt{\sum_k (\sigma_{g,k}^i)^{-2}}$ where i represent the indicator, g the galaxy and k goes over all the measurements for this indicator and galaxy. We get these values for both methods. Then, we compute the uncertainty-weighted mean across all galaxies

$$\bar{\mu}_i = \frac{\sum_g \bar{\mu}_g^i / (\sigma_g^i)^2}{\sum_g 1 / (\sigma_g^i)^2} \quad (6)$$

and its uncertainty $\sigma_{\bar{\mu}_i} = 1/\sqrt{\sum_g (\sigma_g^i)^{-2}}$. We then construct a difference $X_{ij} \equiv \bar{\mu}_i - \bar{\mu}_j$, with uncertainty $\sigma_{X_{ij}} = \sqrt{\sigma_{\bar{\mu}_i}^2 + \sigma_{\bar{\mu}_j}^2}$. This defines X_{ij} for all methods with at least one galaxy in common, which we then use as constraints to infer the $\bar{\mu}_i$. Since not all method pairs have an X_{ij} some

methods will have more constraints than others, leading to better-determined $\bar{\mu}_i$. There is even the possibility of having methods with zero constraints or only one constraint. The former would imply that we cannot determine $\bar{\mu}_i$ for that method while the latter can cause degeneracies in the $\bar{\mu}_i$ of different indicators. It is important to realise that $\bar{\mu}_i$ represents an average relative distance inferred by method i , which must therefore be defined relative to an arbitrary zero-point. We take this to be the mean of all the $\bar{\mu}$. We constrain the $\bar{\mu}_i$ using the NUTS method of Hamiltonian Monte Carlo as implemented in the NumPyro sampler (Bingham et al. 2019; Phan et al. 2019), with wide uniform priors on the $\bar{\mu}_i$, ensuring convergence through the Gelman–Rubin statistic.

4 RESULTS

4.1 NED-D

From the 76 indicators in NED-D, only 66 have at least one galaxy containing either two measurements with that indicator or one with that indicator and one with another. The others, which we cannot analyse for consistency and hence neglect for the remainder of the paper, are **Quasar spectrum**, **SGRB**, **PAGB Stars**, **S Doradus Stars**, **GC K vs. (J-K)**, **CO ring diameter**, **Radio Brightness**, **L(H{beta})-{\sigma}**, **Dwarf Ellipticals** and **Jet Proper Motion**.

To set the stage we show in Fig. 1 the distributions of distances probed by each method we consider. For each method the box shows the median distance (orange bar) and interquartile range, while the whisker covers the full range. The methods are ordered in median distance. We can see that 17 indicators (from **SX Phe Stars** to **Mass Model**) measure median distances lower than 0.1 Mpc. Then, we have seven indicators (from **Miras** to **GC SBF**) having distances from 0.1 Mpc to 1 Mpc and nine from 1 Mpc to 10 Mpc (**Wolf-Rayet** to **PNLF**). These three ranges represent the first rung in the distance ladder. The second rung goes from a few Mpc to around several tens of Mpc (**Wolf-Rayet** to **Black Hole**). The third rung covers ~ 100 Mpc to ~ 400 Mpc. The **SN Ia** method extends to thousands of Mpc, while **GRB** and **HII LF** reach even beyond 10 Gpc albeit with large relative uncertainties ($\gtrsim 30\%$). We also show in red the median fractional uncertainty of all measurements using a given indicator in NED-D, with scale on the right-hand y-axis. The methods highlighted in bold are those that we will find to be most consistent. Most of these have median relative errors lower than 20%, and two even below 10% (**M Stars** and **BL Lac Luminosity**). **BL Lac Luminosity** also probes to several Gpc. To be of maximum usefulness in the distance ladder, an indicator would ideally be self-consistent and consistent with other (good) methods, and probe large distances with small uncertainty.

Our consistency results are summarised in Tables 1 for the standard candle distance indicators and 2 for the standard ruler and secondary indicators. We report, for each method, the number of galaxies that have at least two distance measurements using the given indicator, the number of measurement pairs for these galaxies, the total number of measurements in the NED-D catalogue from this indicator and the number of references reporting these measurements, the

Table 1. Results for the standard candle distance indicators. We present the number of galaxies having at least two measurements by a given method, the number of measurement pairs in these galaxies, the total number of measurements in NED-D along with the number of papers from which these measurements derive, the KLD p -value and external consistency statistics. The p -value is shown in green if it is greater than 0.05 (indicating consistency), orange if it is between 0 and 0.05 (indicating inconsistency), and red if it is 0 (indicating severe inconsistency). In cases of inconsistency, we indicate the p -value after rescaling the uncertainties to a standard half-normal in parenthesis. If this produces consistency, we indicate whether the uncertainties were originally underestimated (downward-pointing arrow) or overestimated (upward-pointing arrow). The final column shows the fraction of other methods with which the method in question is externally consistent, either out-of-the-box, after making the means consistent or after making the uncertainties consistent or both. Methods that are internally consistent and members of the maximal externally consistent set are shown in bold. (See text for full details.)

Distance indicator	# of galaxies	# pairs	# total measurements/references	KL p -value	External consistency
BL Lac Luminosity	2	4	20 / 11	0.9705	1 - 1 - 1 - 1 / 1
RSV Stars	2	4	9 / 6	0.8298	9 - 22 - 27 - 27 / 28
OB Stars	2	2	4 / 3	0.7383	27 - 30 - 30 - 31 / 31
Novae	6	14	18 / 11	0.4382	35 - 40 - 43 - 43 / 46
Miras	6	119	36 / 27	0.1121	20 - 24 - 32 - 32 / 39
RV Stars	1	10	5 / 1	0.0845	6 - 7 - 14 - 14 / 18
Statistical	14	168	292 / 27	0.0795	15 - 22 - 35 - 35 / 54
Brightest Stars	21	127	129 / 41	0.074	21 - 26 - 40 - 40 / 44
M Stars	1	3	6 / 5	0.0686	18 - 24 - 32 - 32 / 33
Delta Scuti	2	29	12 / 2	0.0395 (0.8241) ↑	14 - 16 - 27 - 27 / 31
Horizontal Branch	22	139	110 / 53	0.0037 (0.1495) ↓	19 - 25 - 36 - 36 / 40
PNLF	45	285	183 / 57	0.0016 (0.0019)	23 - 26 - 41 - 41 / 52
AGN time lag	11	13	32 / 3	0.0 (0.7099) ↓	2 - 3 - 6 - 6 / 6
Carbon Stars	7	182	82 / 13	0.0 (0.4555) ↑	25 - 27 - 33 - 33 / 38
Cepheids	115	69496	10956 / 325	0.0 (0.0)	8 - 12 - 26 - 26 / 47
CMD	123	41733	1265 / 170	0.0 (0.0)	15 - 23 - 34 - 35 / 51
GRB	139	1661	729 / 17	0.0 (0.0)	-
GCLF	176	2288	781 / 96	0.0 (0.0)	15 - 21 - 31 - 31 / 40
RR Lyrae	2443	16262	26409 / 216	0.0 (0.0)	16 - 23 - 31 - 32 / 43
Red Clump	24	3420	236 / 63	0.0 (0.0)	16 - 19 - 28 - 28 / 40
SNIa SDSS	1849	7687	6054 / 1	0.0 (0.0)	0 - 0 - 1 - 1 / 4
SZ effect	78	426	283 / 19	0.0 (0.0)	6 - 12 - 15 - 15 / 16
SBF	406	4403	1781 / 67	0.0 (0.0)	19 - 23 - 31 - 31 / 42
TRGB	307	8537	1736 / 336	0.0 (0.0)	15 - 26 - 34 - 35 / 54
Type II Cepheids	7	435	62 / 22	0.0 (0.3613) ↓	18 - 24 - 40 - 40 / 44
SNIa	4978	129581	30843 / 140	0.0 (0.0)	10 - 14 - 22 - 22 / 38
AGB	0	0	2 / 2	-	22 - 23 - 23 - 23 / 23
B Stars	0	0	2 / 2	-	28 - 28 - 28 - 28 / 30
Black Hole	0	0	17 / 2	-	4 - 6 - 10 - 11 / 11
Blue Supergiant	0	0	2 / 1	-	11 - 12 - 25 - 25 / 25
BCG	0	0	239 / 1	-	9 - 9 - 11 - 11 / 11
FGLR	0	0	7 / 7	-	9 - 15 - 21 - 21 / 21
GC SBF	0	0	3 / 1	-	13 - 14 - 18 - 18 / 19
HII LF	0	0	17 / 2	-	6 - 11 - 12 - 12 / 15
SX Phe Stars	0	0	3 / 2	-	10 - 11 - 13 - 13 / 13
Subdwarf fitting	0	0	1 / 1	-	19 - 22 - 22 - 22 / 22
SNIi radio	0	0	24 / 2	-	3 - 9 - 15 - 16 / 17
White Dwarfs	0	0	1 / 1	-	21 - 22 - 21 - 22 / 22
Wolf-Rayet	0	0	1 / 1	-	0 - 3 - 5 - 5 / 5
Grav. Wave	0	0	8 / 8	-	4 - 4 - 4 - 4 / 4

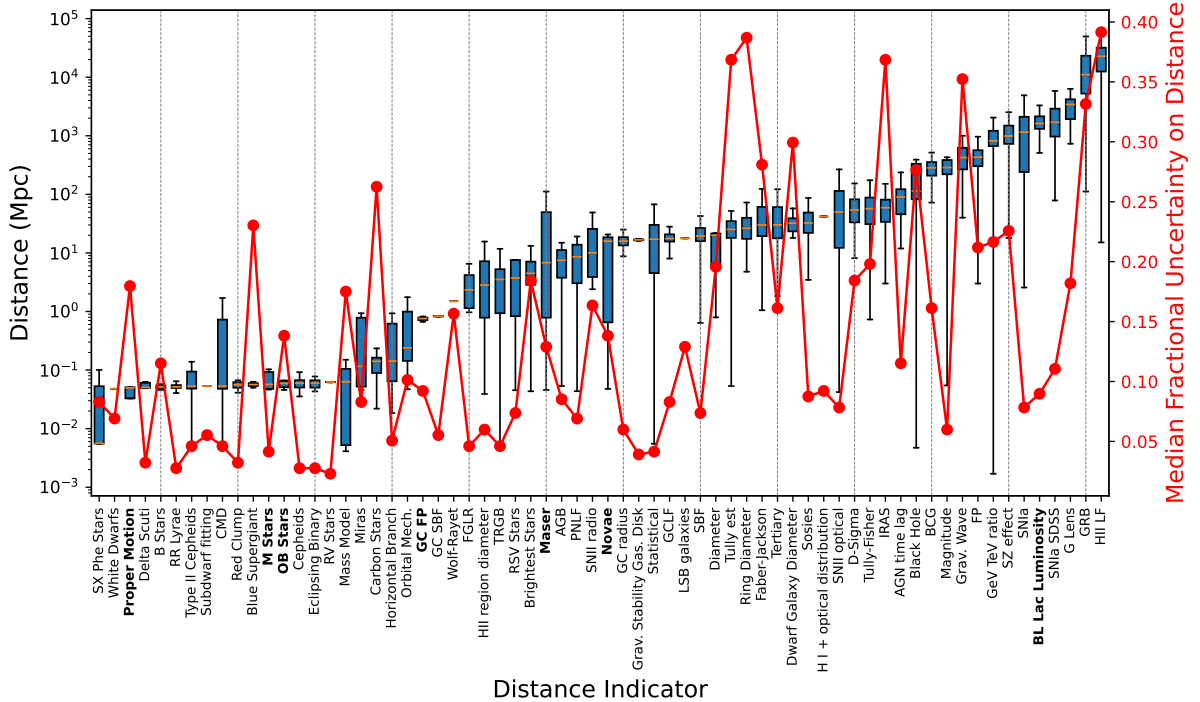
KLD p -value (with a traffic-light-style colouring indicating the severity of the inconsistency) and external consistency statistics. For self-inconsistent cases we show the p -value after rescaling the uncertainties to give Δ_{ij} the variance of a standard half-normal distribution in parentheses. The final column contains the number of other distance indicators with which the method in question is consistent ($p > 0.05$), in four different hyphen-separated cases. The first number describes the fiducial case with no shifting of means or rescaling of uncertainties. The second number reports the result when the means of the μ distributions are made to coincide, thus eliminating discrepant central values as a cause of inconsistency.

The third number corresponds to rescaling the uncertainties so that the Δ_{ij} distribution has the width of a standard half-normal by construction, eliminating discrepant uncertainties as a cause of uncertainty. The fourth number corresponds to the case with both shifted means and rescaled uncertainties, eliminating both of these as possible causes. The final number is the total number of other methods with which that method has overlap, i.e. the largest number of pairs that could possibly be consistent.

Tables 1 and 2 show that most of the NED-D distance indicators are internally inconsistent, largely for an unidentified reason. This indicates that the catalogued distances are sub-

Table 2. As Table 1, but for standard ruler (above the horizontal line) and secondary (below the line) distance methods.

Distance indicator	# of galaxies	# pairs	# total measurements/references	KL p -value	External consistency
Proper Motion	1	6	5 / 3	0.8918	24 - 26 - 29 - 30 / 32
Maser	6	29	24 / 20	0.6253	28 - 32 - 35 - 36 / 36
Dwarf Galaxy Diameter	8	8	16 / 1	0.0004 (0.582) \uparrow	17 - 17 - 21 - 21 / 21
G Lens	15	70	86 / 14	0.0002 (0.6975) \downarrow	1 - 1 - 3 - 3 / 3
Eclipsing Binary	49	3397	273 / 48	0.0 (0.0007)	22 - 23 - 34 - 34 / 42
HII region diameter	19	25	53 / 7	0.0 (0.0261)	7 - 20 - 42 - 42 / 42
Ring Diameter	47	47	212 / 1	0.0 (0.2025) \uparrow	10 - 11 - 18 - 18 / 18
SNII optical	309	6090	1622 / 89	0.0 (0.0)	17 - 22 - 32 - 32 / 42
GC radius	0	0	101 / 8	-	22 - 25 - 34 - 34 / 37
Grav. Stability Gas. Disk	0	0	2 / 1	-	1 - 3 - 4 - 4 / 4
Orbital Mech.	0	0	3 / 3	-	20 - 22 - 22 - 22 / 22
GC FP	1	3	3 / 3	0.2469	16 - 17 - 18 - 19 / 19
GeV TeV ratio	4	8	30 / 11	0.0385 (0.7002) \downarrow	1 - 1 - 1 - 1 / 1
Faber-Jackson	427	1947	1424 / 6	0.0101 (0.6445) \uparrow	5 - 10 - 25 - 25 / 29
Diameter	3	3	6 / 2	0.0089 (0.0504) \uparrow	18 - 20 - 26 - 26 / 31
D-Sigma	551	2901	1995 / 9	0.0 (0.0)	9 - 12 - 14 - 14 / 25
FP	967	1675	130214 / 22	0.0 (0.0)	10 - 13 - 19 - 19 / 28
IRAS	405	640	2947 / 2	0.0 (0.0)	4 - 5 - 20 - 21 / 35
Mass Model	2	4	7 / 7	0.0 (0.8942) \downarrow	0 - 1 - 10 - 10 / 10
Tully-Fisher	9107	231663	56436 / 78	0.0 (0.0)	13 - 24 - 31 - 32 / 48
H I + optical distribution	0	0	1 / 1	-	0 - 1 - 1 - 1 / 1
LSB galaxies	0	0	2 / 1	-	7 - 8 - 9 - 9 / 10
Magnitude	0	0	111 / 3	-	13 - 31 - 38 - 38 / 40
Sosies	0	0	287 / 3	-	10 - 12 - 20 - 20 / 21
Tertiary	0	0	284 / 4	-	6 - 11 - 14 - 14 / 22
Tully est	0	0	1434 / 1	-	17 - 17 - 28 - 28 / 41


Figure 1. Whisker plot showing the full range (whiskers) and interquartile range (boxes) of the distances probed by each indicator in NED-D. The median distances are shown by orange bars. We also show the median fractional distance uncertainty of each method in red, with scale on the right-hand y-axis.

ject to problems like systematics and statistical outliers and are likely unsuitable for precision analyses such as constraining the Hubble constant. Indeed, the methods normally used for inferring H_0 —Cepheids, TRGB and SNIa—are among the methods with the highest number of measurement pairs and all have a consistency p -value of 0. We also show the results for only the measurements that can be standardised, i.e. the ones with a quoted value for either H_0 or μ_{LMC} . These results are shown in Appendix A (Figs. 1 and A1), where we see for example that the CMD method becomes much better behaved.

For internal inconsistency, we show with an arrow whether the inconsistency indicates under- or overestimated uncertainties. Some indicators present underestimated uncertainties (Horizontal Branch, AGN time lag, Type II Cepheids, G Lens, HII region diameter, GeV TeV ratio, and Mass Model) while Delta Scuti, Carbon Stars, Dwarf Galaxy Diameter, Ring Diameter, Faber-Jackson and Diameter are the opposite. For the remainder ones, the cause of the inconsistency was not the inconsistent uncertainties. Some distance indicators have external consistency results but no internal consistency p -value because they have at most one distance measurement to any given galaxy. One indicator (GRB) has an internal consistency result but no external consistency results because all of its measurements are to galaxies having no distances by any other method.

In Fig. 2 we summarize the results for all distance indicators. We show the p -values both for internal consistency along the diagonal and external consistency on the off-diagonal. Cases where no consistency test is possible due to no overlap in measurements are shown as empty squares. Green indicates consistency ($p > 0.05$), while p -values below 0.05 are shown by the colour-bar, with darker red indicating lower p . As we use 10,000 mocks the p -value is calculated in units of 0.0001; anything below this (i.e. no mock KLD as large as that of the data) is shown in dark red. The hatching indicates the cause of inconsistency. Over- and underestimated uncertainties are shown by forward and backward slanting diagonal lines respectively, while inconsistent means are shown by the circle pattern. Note that some comparisons exhibit both problems and hence have both types of hatching. If neither shifting the means nor rescaling the uncertainties removes the inconsistency we label it “essentially”, indicated by no hatching.

Figure 2 contains all the information for the consistency of the distance indicators. The total number of consistent cases is 427. 219 are inconsistent due to have uncertainties that are either too large or too small (mostly too small). Six have inconsistent means, and 169 have both problematic means and uncertainties. For problems that our tests cannot detect such as combinations of the previous ones along with e.g. outliers or non-Gaussian behaviour, we show no hatching. There are 169 such cases. Finally, 1994 pairs have no shared galaxies and hence no p -value. Therefore, the analyses showing consistency are 427 out of 932, representing 41.8% of all cases. Combining consistent cases with those where we have identified the problem yields 821 cases, representing 88.1% of the total. Hence, even though most distance indicators are internally inconsistent, close to half of the cross-analyses are consistent, while around just one tenth are inconsistent with a non-obvious problem.

In Fig. 3, we present the percentage of inconsistent

Table 3. As Table 1 but for the SH0ES 2022 catalogue. In this case all distances use the Cepheid method so there is no notion of external consistency. N3982 and N0691 are shown in orange to indicate that they would fail a two-tailed consistency test (their Δ_{ij} values form a distribution more similar to a standard half-normal than would be expected from statistical noise under the assumption of consistency between all the measurements).

Name	Measurement pairs	KL p -value
Full dataset	345615	0.6613
N4258	97903	0.6896
LMC	115921	0.1286
N3982	406	0.9992
N0691	153	0.9808
N7541	120	0.953
N2442	2628	0.933
N1015	1378	0.8774
N7329	528	0.7556
U9391	528	0.7356
N4639	55	0.661
N7678	528	0.6108
N0105	378	0.553
N5468	13530	0.5328
N5643	190	0.5194
N1448	5995	0.464
N5728	820	0.4522
N3583	1326	0.4354
N4680	4278	0.4062
N4536	435	0.3974
N3147	1128	0.3972
N4424	780	0.3938
N3972	351	0.2766
N1309	1035	0.2418
N2525	231	0.1936
N3021	351	0.1834
M101	33411	0.1768
N5917	210	0.1756
N5861	91	0.149
N3370	5050	0.1276
N2608	120	0.1174
N1365	2628	0.117
Mrk 1337	105	0.1142
N3254	2628	0.0778
N1559	15576	0.042 (0.587) \uparrow
N3447	1431	0.0242 (0.2722) \uparrow
N5584	31375	0.0196 (0.851) \uparrow
N0976	28	0.0166 (0.4116) \downarrow
N7250	465	0.0154 (0.6016) \downarrow
M31	1485	0.015 (0.643) \downarrow
N4038	36	0.0004 (0.1314) \downarrow

method pairs and of fully externally consistent methods. This is shown as a function of the number of discarded or remaining methods (see Sec. 3.2), where it is assumed that each discarded method is responsible for inconsistency in any pair in which it is present. We continue discarding methods until we obtain the maximum set of fully externally consistent methods. We find this set to contain the following 18 methods: AGN time lag, PNLF, Sosies, M Stars, LSB galaxies, Proper Motion, Novae, SX Phe Stars, Maser, Dwarf Galaxy Diameter, GC FP, Subdwarf fitting, OB Stars, Orbital Mech. , B Stars, AGB, BL Lac Luminosity, GeV TeV ratio. It is

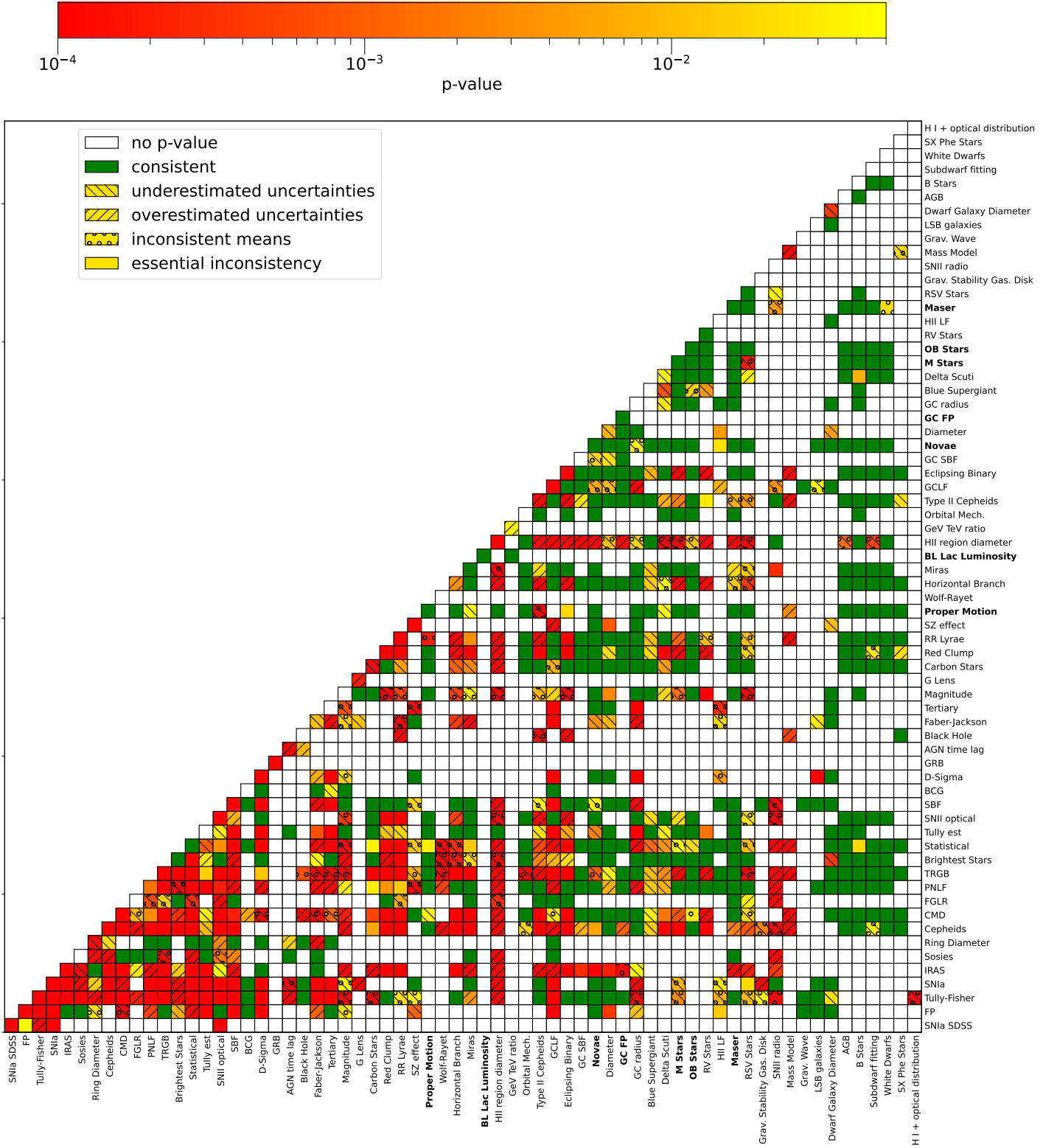


Figure 2. Consistency p -value results for the NED-D distance indicators. The diagonal squares describe internal consistency whereas the non-diagonal squares describe external consistency with other methods. We show the cases with p -value higher than 0.05 (i.e. not rejecting the null hypothesis) in green, the cases with no reported p -value in white and the cases with a p -value lower than 0.05 in a logarithmic colour scale. We show cases with underestimated uncertainties with a backslash hatching, overestimated uncertainties with forward-slash hatching, and inconsistent means with circle hatching. If the cause of the inconsistency is neither one of these nor their combination we show no hatching. We call this an essential inconsistency.

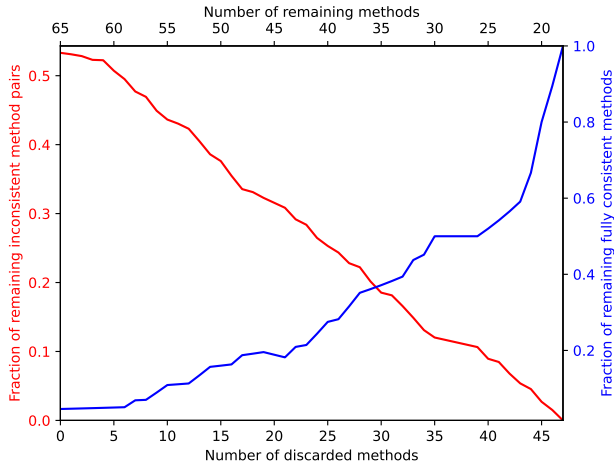


Figure 3. *Red:* number of inconsistent method pairs (having $p < 0.05$) as a function of the number of discarded or remaining methods, assuming that discarded methods are responsible for inconsistency in all comparisons involving them. *Blue:* number of fully consistent methods (having 100% external consistency) as a function of the number of discarded methods. We also show the total number of methods remaining on the top axis.

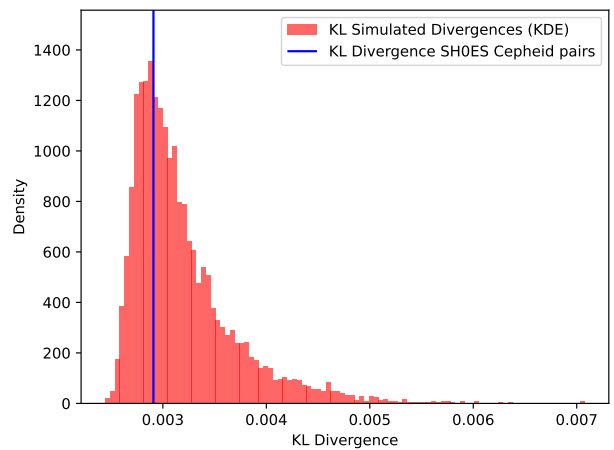
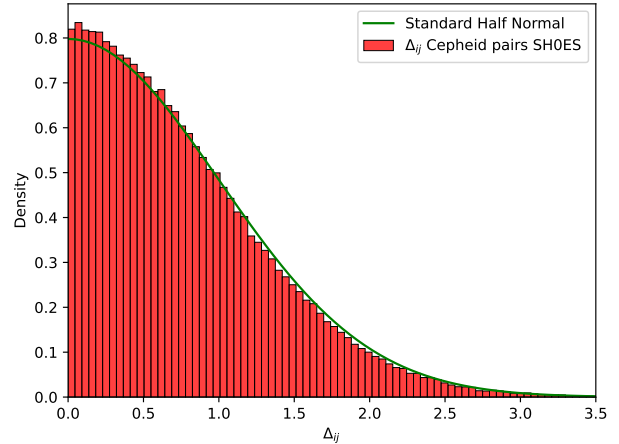


Figure 5. *Top:* Normalized probability distribution function (pdf) of the difference in units of Δ_{ij} for the SH0ES 2022 catalogue. We show the theoretical pdf of the standard half-normal for comparison. *Bottom:* Histogram for the mock KLD values generated under the null hypothesis of consistency compared to the KLD value of the real data.

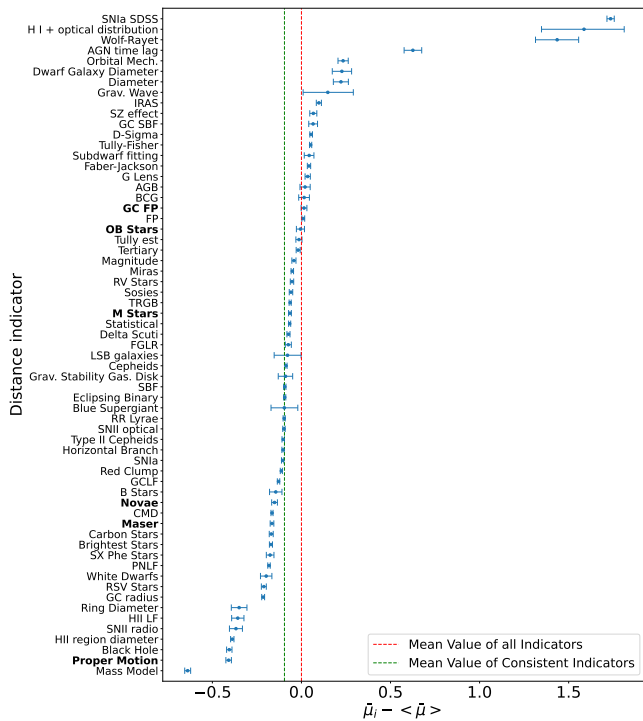


Figure 4. Mean values and 1σ C.L. uncertainties for the average distance modulus $\bar{\mu}$ returned by each indicator relative to the mean of all. Negative values correspond to distances underestimated on average relative to the mean of all indicators and vice versa.

interesting to compare this with the set of 12 self-consistent methods: **BL Lac Luminosity, RSV Stars, OB Stars, Novae, Miras, RV Stars, Statistical, Brightest Stars, M Stars, Proper Motion, Maser, GC FP.** The intersection of these sets gives us a set of 7 methods simultaneously achieving perfect internal and external consistency, which we highlight in bold throughout the paper: **M Stars, Proper Motion, Novae, Maser, GC FP, OB Stars, BL Lac Luminosity.** If we showed Fig. 2 with only these indicators, all the non-empty squares would be green.

The maximum set of fully externally consistent methods is not the same as the set of self-consistent methods. The set of methods being fully externally consistent but self-inconsistent contains 11 methods: **AGN time lag, PNLF, Sosies, LSB Galaxies, SX Phe Stars, Dwarf Galaxy Diameter, Subdwarf fitting, Orbital Mech., B Stars, AGB, GeV TeV ratio.** On the other hand, the set of methods being self-consistent but not fully externally con-

sistent contains 5 methods: **RSV Stars**, **Miras**, **RV Stars**, **Statistical**, **Brightest Stars**. It is interesting to see that being fully externally consistent does not guarantee being internally consistent. This can be caused by a consistent subset of an indicator agreeing with other distance indicators or by both indicators being inconsistent in a way that cancels out when they are compared.

In Fig. 4, we present a whisker plot for the mean value and minimum 1σ C.L. uncertainties for the constraints on $\bar{\mu}_i$, a measure of the overall distance modulus returned by each method relative to the average of all of them. We present them in order for visual clarity. We discard two indicators (**BL Lac Luminosity** and **GeV TeV ratio**) as they both had only one constraint equation, which linked them (i.e. they each overlapped with only one other method in one galaxy, and that method for one of this pair was the other). This causes a perfect degeneracy between their $\bar{\mu}$ values, making the marginalised posteriors unbounded.

Fig. 4 shows the methods that tend to overestimate and underestimate distance modulus in average. **Mass model** is the indicator with the strongest underestimation having a difference $\Delta\bar{\mu} \equiv \bar{\mu}_i - \langle\bar{\mu}\rangle \approx -0.6$ which corresponds to an underestimation of the luminosity distance by $\sim 20\%$. **Proper Motion**, **Black Hole**, **HII region diameter**, **SNII radio**, **HII LF**, and **Ring Diameter** have a difference of lower than -0.25 implying underestimation of the distance relative to the mean by more than 10% . Three indicators (**SNIa SDSS**, **H I + Optical distribution** and **Wolf-Rayet**) have a difference of around 1.5 and higher, representing an overestimation of distance relative to the mean by a factor of around 2 or more. If we look for these indicators in figure 2, we can see that they are not consistent in any of the analyses. This is expected since they appear to overestimate distances by a huge margin. **AGN time lag** shows a difference higher than 0.5 implying an overestimation of distances higher than 25% . Out of the 7 indicators achieving full external consistency and internal consistency, only one seems to be significantly misestimating distances relative to the mean: **Proper Motion**. The remainder of the fully consistent indicators return values close to the mean (**BL Lac Luminosity** has no constraint due to the perfect degeneracy with **GeV TeV ratio**). Note that of course the mean may be biased by inconsistent methods, so returning distances compatible with the mean is not a reliable indicator of a method's quality.

4.2 SH0ES

We now move to the analysis of the independent SH0ES 2022 catalogue. Fig. 5 presents two histograms for this catalogue. The upper panel shows the normalized pdf of the differences between the distance moduli (Δ_{ij}) and the comparison to the standard half-normal. The lower panel shows the histogram of KLD values over the 10000 mock datasets compared to the value in the real data (vertical blue line). The full results are shown in Table 3, which (except for the first row describing the full catalogue) contains the galaxy name, number of measurement pairs and KLD p -value. The first two galaxies (N4258 and LMC) are in the first rung of the distance ladder and are used to calibrate the Cepheid PL relation by means of geometric distances to those galaxies.

Fig. 5 and the top row of Table 3 indicate that the SH0ES

2022 catalogue agrees well with the null hypothesis of statistical consistency. The two galaxies used for the first rung that calibrates the PL relation are also consistent with the null hypothesis. It is particularly important for these to be consistent, as inconsistency there would propagate into all the other distances and hence the constraint on e.g. H_0 . From the 38 galaxies in the second rung (M31 does not host a SNIa but it is included in the SH0ES catalogue), 31 are consistent while the remaining 7 are inconsistent due to underestimated uncertainties. The inconsistency is in most cases weak; had we take a tighter 0.01 threshold for the p -value, only one galaxy would have been inconsistent (N4038). Most of the inconsistent galaxies have <2000 pairs (apart from N1559 and N5584) and hence play a relatively small role in the consistency of the whole catalogue and the calibration of M_B^0 and hence H_0 . Four of the seven inconsistent galaxies have underestimated uncertainties (N0976, N7250, M31 and N4038) whereas N1559, N3447 and N5584 have overestimated uncertainties. Interestingly, the inconsistent galaxies having more than 15000 measurement pairs have overestimated uncertainties, which has the effect of overestimating the uncertainty on H_0 . We highlight two galaxies in lighter orange (N3982 and N0691) that would be inconsistent under a two-tailed test due to having $p > 0.975$. This is due to the KLD being surprisingly low relative to the mock data distribution, indicating that the data conforms more closely to a standard half-normal than would be expected under the assumption of consistency given the uncertainties.

To study the effect of the inconsistent galaxies on the constraints on H_0 in SH0ES, we repeat the MCMC inference described in Sec. 2.2 but removing the seven inconsistent galaxies. These are all second-rung or non-SNIa host galaxies. The new constraint on the Hubble constant is $5 \log_{10} H_0 = 9.319 \pm 0.032$, or $H_0 = 73.08^{+1.07}_{-1.08}$ km/s/Mpc in comparison to the baseline result with all galaxies of $5 \log_{10} H_0 = 9.318 \pm 0.031$, or $H_0 = 73.04 \pm 1.01$ km/s/Mpc. Both are at a 5σ C.L. tension with Planck 2018. This is a negligible change from the case with all galaxies included, showing that the Hubble tension does not result even in part from these galaxies with inconsistent Cepheid distances.

5 DISCUSSION

5.1 Implications of the results

Our main result is that many of the distance measurements in NED-D are subject to significant problems, including “unknown unknowns” such as unaccounted-for systematics and outliers as well as the “known unknowns” of misestimated uncertainties and inconsistent central distance values between indicators. This makes it challenging currently to use for inference of cosmological parameters; the only previous attempt to do so yielded a 21% precision estimate of H_0 (70 ± 15 km/s/Mpc) from an ensemble of estimates and galaxies comparable to that studied here (Steer 2020). This is likely sufficiently low precision not to be significantly affected by the inconsistencies we identify here. Despite our results, NED-D provides an excellent starting point to build a robust set of distance ladder measurements for cosmological inference. This would be similar to the approach of collaborations like SH0ES that construct and employ smaller, more carefully

curated—and hence more self-consistent—extragalactic distance datasets.

Indeed, we find the Cepheids in the SH0ES 2022 catalogue not to exhibit significant problems. This supports the findings of [Riess et al. \(2022\)](#) that the dispersion in the Cepheid measurements agrees with the fiducial uncertainties without any unexplained variance. However, it is important to note that our test is not sensitive to constant shifts in the distance modulus across all Cepheids in a given galaxy. This would leave the distance modulus difference between the Cepheids, Δ_{ij} , unchanged. This effect could in principle be present if the Wesenheit relative magnitude m_H^W or the fiducial Wesenheit absolute magnitude $M_{H,1}^W$ have an unaccounted-for constant systematic error. Such a global shift to the distance modulus to each Cepheid could alter the Hubble diagram arbitrarily when combined with SNIa.

There is a small set of methods that exhibit both internal and external consistency (**M-stars luminosity**, **Novae**, **Masers**, **Globular Cluster Fundamental Plane**, **O- and B-type Supergiants**, **BL Lac Luminosity** and **Proper Motion**). However all of these have a small number of measurement pairs (no more than 127), and hence would not afford good constraints on the distance ladder—or cosmological parameters derived therefrom—in their own right. A worrying observation in this regard is that it is harder to acquire sufficient evidence to reject the null hypothesis when the dataset is smaller, suggesting that these methods may also become classified as inconsistent as more data on them is collected.

It is important to emphasize that statistically consistency is a necessary but not sufficient condition for a method to be useful in the distance ladder. Another necessary condition is to have a sufficient number of measurements to bring significant constraining power. For this reason, the seven methods in our fully consistent set are inferior to others having many more measurements like **Cepheids**, **CMD**, **RR Lyrae**, **TRGB**, **Tully-Fisher** and others. Future work must therefore either focus on statistically consistent subsets of these methods, or develop ways of measuring distances using the methods we identifying as having naturally higher consistency to more galaxies. An interesting indicator in this regard is **Faber-Jackson**, which has a very high number of measurement pairs (1947) and a p -value of 0.0101, near the threshold for consistency. We see from Table 1 that the inconsistency is due to overestimated uncertainties, probably the least pernicious cause. Another interesting case is **CMD**, which is self-consistent when only taking the measurements standardised through H_0 or μ_{LMC} (Appendix A). Moreover, this indicator has 3454 measurement pairs, almost double **Faber-Jackson** when restricting to standardisable measurements. It therefore shows promise as a useful method for constraining the distance ladder in the future.

Containing as it does measurements collected over 40 years, it is perhaps unsurprising that the overall consistency of NED-D is low. To investigate this further, we try splitting some of the better-known methods with many measurements (**Cepheids**, **TRGB**, **SNIa**, **RR Lyrae**, **CMD** and **Tully-Fisher**) into three bins of measurement year with roughly equal numbers of measurements in each bin and calculating the p -value for self-consistency within each bin. In this way, we can see if there are signs of an improving consistency over time. However, we find that for all indicators and

bins the p -value remains, with the sole exception of **RR Lyrae** which has a p -value of 0.0008 for the intermediate bin. This indicates that the inconsistencies are not solely due to poorer measurements in the past or discrepancies between analysis choices in the past versus more recently.

Some of the inconsistency derives from non-independent measurements. For example, NED-D includes three TRGB distances to N6822 from [Fusco et al. \(2012\)](#), yet two of these differ only in the TRGB calibration, not the measurements themselves, and the third is an average of these two. This is simple a limitation with the way the literature was trawled to compile the catalogue: the abstract of the paper itself presents just one independent measurement. Another example comes from [Rich et al. \(2014\)](#), where the distances to 39 Cepheids in the galaxy NGC 6822 are provided. However, six of them were excluded from the analysis in the paper due to problems like phase shifting, crowding and deviations from the PL relation. Yet all 39 measurements are included in NED-D, potentially contributing significantly to inconsistency.

By excluding these problematic and non-independent measurements, we would get more information on the possibility of reducing the inconsistency across NED-D. One way to do this might be to automate a search over the literature using an Artificial Intelligence Large Language Model (LLM) as opposed to the human searchers employed in the construction of NED-D. This could allow a pre-cleaning of the data capable of removing unreliable cases. The LLM could also potentially be used to homogenise the calibrations of the methods by identifying the anchor used in a given paper, and its assumed distance, and then rescaling the measurements appropriately. If the inconsistencies could be reduced sufficiently, enormously more measurements—from a great deal more distance indicators—could be used to calibrate the distance ladder for cosmological inference and other applications.

Our results could potentially help explain the Hubble tension. For example, Fig. 4 indicates that Cepheid distances are lower than the mean of all methods. If distance were underestimated in SNIa host galaxies, then, by $H_0 \approx cz/D$, the Hubble constant would be overestimated. TRGB likewise produce distances below the mean. Note however that the mean of all methods (most of which are inconsistent) is not a reliable indicator of the truth, and this simple accounting neglects the possibility of *relative* differences between the calibrator and cosmological first-rung samples.

To close this subsection we briefly describe the physics of the methods that we find to be most consistent, achieving both internal and external consistency. **M-stars luminosity** uses a relationship between the absolute magnitude of red dwarf stars and the temperature-independent spectral index. However, it requires low-resolution spectroscopy and thus it can only be applied in nearby galaxies, like the LMC ([Schmidt-Kaler & Oestreich 1998](#)). The **Novae** standard candle comes from a relation between the absolute magnitude at the maximum and the rate of decline in the flux known as the MMRD relation ([Della Valle & Livio 1994](#)). For **O- and B-type Supergiants** stars, there exists a relation between their absolute magnitude and their spectral type and luminosity class. This method was notably applied to 30 Doradus nebula in the LMC ([Walborn & Blades 1997](#)). **BL Lac Object Luminosity** is a method based on calibrating the absolute magnitude of BL Lacertae objects. It was found that the dispersion of this is small, although standardising it ro-

bustly does require a K-correction and evolution correction (Sbarufatti et al. 2005).

The **Maser** standard ruler is based on the dynamics of a water maser in an accretion disk surrounding a supermassive black hole. Using Very Long Baseline Interferometry (VLBI) it is possible to determine individual maser spots, the velocity of the masers and the shape of the disk. The physical size can then be deduced from Kepler’s laws and the angular size, affording a determination of the angular diameter distance (Humphreys et al. 2004; Reid et al. 2019). The **Globular Cluster Fundamental Plane (GCFP)** relates velocity dispersions, radii, and mean surface brightness of globular clusters to their absolute magnitude. This has been used to determine the distance to M31 (Strader et al. 2009). Finally, the **Proper Motion** method compares a galaxies’ apparent motion on the plane of the sky to its absolute motion calculated dynamically. This is also only applicable locally where proper motions are measurable (e.g. Lépine et al. 2011).

5.2 Comparison with the literature

Our NED-D analysis builds upon Singh (2021), where possible evidence for systematic underestimation of distance uncertainties was found. This could imply strong systematics on the late-time measurements of H_0 , for example (Freedman et al. 2019a; Riess et al. 2022; Anand et al. 2022; Scolnic et al. 2023; Riess & Breuval 2024), which might overestimate the tension with *Planck*. However, as mentioned before, Singh (2021) uses a non-symmetric expression for the discrepancy between two measurements that does not include the uncertainty of both measurements. This is in contrast to the Mahalanobis distance (Eq. 3) which takes both of them into account. The non-symmetric expression gives higher sigma differences as one of the uncertainties is neglected, artificially increasing discrepancies. Even so, in agreement with Singh (2021) we infer inconsistencies in most of the NED-D methods.

The NED-D catalogue has been used in various ways. For example, Cappellari et al. (2011) estimated uncertainties in the distances to galaxies in the ATLAS3D sample estimated from a Virgocentric infall peculiar velocity model by correlating them against the direct measurements in NED-D. This produced a sizeable 27% distance uncertainty for 692 galaxies with at least one NED-D distance measurement. Ohlson et al. (2023) used NED-D along with the Local Volume Galaxy catalogue (Karachentsev et al. 2013) to create a catalogue of galaxies within 50 Mpc with known distances, to study for example their nuclear X-ray activity.

NED-D has also been used to constrain fifth forces induced by modified gravity. Desmond et al. (2019) used the measurements of 51 galaxies with Cepheids and TRGBs from NED-D to set a bound on ΔG , an effective change to Newton’s constant due to a long-range fifth force. This test assessed only *relative* consistency between Cepheid and TRGB distances as a function of ΔG , although we see from Fig. 2 that these indicators are essentially inconsistent in NED-D. The consistency may be worse under modified gravity, but it is not good under General Relativity. Similarly, Desmond et al. (2021) used the TRGB distance to the LMC from NED-D as a constraint in inferring the gravitational constant in this dwarf galaxy from the dynamics of Cepheids in detached eclipsing binary systems. Each of these studies may be impacted by the incon-

sistencies we unearth here, and modified gravity constraints based on direct distance comparisons is a topic we will revisit in future work.

Our SH0ES analysis is complementary to others studying possible systematics and model misspecification in the Cepheid–SNIa determination of H_0 . For example, the error bars on H_0 are impacted by outliers present in the data (Becker et al. 2015). This has been addressed in more recent work by removing the Cepheids that differ from 3.3σ in the global fit of the PL relation, which represent 1.2% of the catalogue (Riess et al. 2022). Another potential systematic is an environment-dependence on SNIa absolute magnitude, in the sense that SNIa in locally star-forming environments are dimmer than those in passive environments (Rigault et al. 2015, 2020). Another consideration is a possible difference between Cepheid observations and data reduction in the more nearby anchor galaxies (MW or LMC) relative to farther away ones like N4258. This can be studied by using only N4258 as the anchor (Kushnir & Sharon 2024). This possibility seems less likely in light of our tests assessing consistency in individual galaxies, in particular the finding that both the LMC and N4258 have internally consistent Cepheid distances. The inferred value of H_0 can also be passband-dependent, with (Uddin et al. 2024) suggesting lower values in the B-band relative to the H-band used in SH0ES. Finally, the James Webb Space Telescope (JWST) has provided new insights on the possible systematics in the distance ladder. In particular, it has been claimed that JWST validates the HST distance measurements in N4258 and five SNIa hosts, rejecting at high significance the possibility of unrecognized crowding of Cepheid photometry growing with distance (Riess et al. 2024a). Indeed, some early samples of JWST Cepheid distances calibrated with only N4258 agree at with their HST counterparts (Jang et al. 2022; Riess et al. 2024b).

Nevertheless there is a plethora of possible problems with the Cepheid distance ladder (Owens et al. 2021, 2022; Madore & Freedman 2024b; Owens et al. 2024; Madore & Freedman 2024a), as well as results from the Chicago-Carnegie Hubble Program (CCHP) using new data from the James Webb Space Telescope (JWST) indicating that $H_0 \approx 70$ km/s/Mpc with an insignificant tension with *Planck* (Freedman et al. 2024). This agrees with earlier CCHP results based on TRGB (Freedman et al. 2019a), and includes distances measured by the novel J-region Asymptotic Giant Branch (JAGB) method which boasts a number of advantages over Cepheids and TRGB (Madore & Freedman 2020; Lee et al. 2024).

6 CONCLUSIONS

We study the consistency of 66 different methods for estimating redshift-independent distances from the NASA/IPAC Extragalactic Database of Distances (NED-D; Steer et al. 2016) and SH0ES 2022 (Riess et al. 2022) catalogues. This is achieved by selecting galaxies that have at least two distance measurements by a given method (“internal consistency”) or at least one measurement by each of two different methods (“external consistency”). We use the Mahalanobis distance to compute the distance differences in units of sigma, forming a distribution for each consistency test. If the distance estimates are consistent (scattered from a common value by their

quoted uncertainties), this distribution should form a standard half-normal. To test if this is the case, we compute the Kullback–Leibler (KL) divergence of the empirical distribution and of 10,000 realizations of random samples under the null hypothesis of consistency and according to the measurements’ uncertainties. We compute the p -value as the fraction of realisations with a KL divergence higher than the value in the real data, adopting a threshold of 0.05 to discard the null-hypothesis of consistency. This indicates under- or over-estimated uncertainties, inconsistent means, statistical outliers, non-Gaussian uncertainties and/or systematic errors. We perform a similar analysis for the SH0ES 2022 catalogue.

For NED-D we find that only 12 distance indicators achieve internal consistency. The maximal set of perfectly *externally* consistent methods has size 18 (i.e. all methods in this set are consistent with each other). The intersection of both sets gives the seven most reliable methods, which are both internally and externally consistent; these are **M Stars luminosity, Proper Motion, Novae, Maser, Globular Cluster Fundamental Plane, O- and B-type Supergiants and BL Lac Object Luminosity**. However, their number of measurements with these methods is low, generally $\mathcal{O}(10)$. This makes them unsuitable for a reconstruction of the distance ladder as they currently stand. A necessary condition besides statistical consistency for usefulness in the distance ladder is having a high number of measurements, and thus a better approach than focusing on these methods may be to build a consistent subset of distances using the indicators that provide many measurements. This paper gives a starting point for such constructions.

We also calculate the average measured distance modulus of each indicator across all galaxies relative to the mean of all indicators. We find that from the best set of indicators, **Proper Motion** is the only one with a considerable discrepancy in average returned distance (17.1% underestimation) relative to the mean. Outside the set of best indicators, some overestimate the luminosity distances by more than 95%; these are **SNIa SDSS, H I + optical distribution and Wolf-Rayet. AGN time lag** shows an overestimation higher than 25% and **Mass model** an underestimation higher than 20%. This indicates that some distance methods in NED-D are strongly affected by systematics and thus unsuitable for cosmological studies. We perform 932 analyses in total, including both internal and external consistency, of which 427 are consistent (41.8% of the total and 12 of them are from internally consistency analyses and the remainder externally consistency analyses). We repeat the analyses for the inconsistency cases by shifting the means and rescaling the uncertainties and find that 394 cases are consistent after these modifications. In the remaining $\sim 1/10$ of cases the inconsistency is not due just to incorrect central values or uncertainties and we cannot identify the cause.

The SH0ES 2022 catalogue exhibits better behaviour. The KL divergence of the full catalogue yields a p -value of 0.66, in agreement with the null hypothesis of consistency. There is thus no evidence for hidden systematics in the Cepheid distances of this catalogue. We repeat this analysis for each of the 40 galaxies in the catalogue separately. The two galaxies in the first rung (N4258 and LMC) that calibrate the PL relation have consistent p -values as well (0.69 and 0.13). This is crucial because an inconsistency in the first rung would propagate to the second and third rungs, potentially biasing

the entire distance ladder. From the second-rung galaxies, we find that 7 out of the 38 present an inconsistency ($p < 0.05$) in a one-tailed test, and 8 in a two-tailed test. These galaxies however play a relatively minor role in the calibration of the SNIa absolute magnitude for which the catalogue was designed. We show this by repeating the MCMC excluding these inconsistent galaxies, finding very similar H_0 .

In summary, the NED-D distance indicator measurements are subject to problems like systematics, outliers, non-Gaussian behaviour and misestimated uncertainties. This is perhaps unsurprising given the heterogeneity of the measurements included, going back ~ 45 years. Thus the full catalogue is not suitable for construction of a robust distance ladder. Even so, several papers have used the NED-D data for studies in cosmology (Freedman et al. 2019b; Chaparro-Molano et al. 2019; Steer 2020; Zaninetti 2023). This shows that by selecting a reliable subset of distances, it is possible to determine galaxies’ distances accurately. Some of the inconsistency comes from non-independent and unreliable distance measurements that were impossible to exclude in the search procedure used to construct the catalogue. By removing these problematic data, the overall consistency might be considerably enhanced, enabling cosmological analysis; we will report elsewhere on our attempts in this direction. The more homogeneous and quality-controlled SH0ES 2022 catalogue, however, has no significant evident problems. We hope the framework devised here will contribute to the future construction of a multiply cross-checked and fully robust distance ladder employing a range of methods.

DATA AVAILABILITY

The NED-D data is available at <https://ned.ipac.caltech.edu/Library/Distances/>, and the SH0ES 2022 data at <https://github.com/PantheonPlusSH0ES/DataRelease>. We will make our code publicly available on publication of the paper. Other data underlying the article may be made available upon request to the authors.

ACKNOWLEDGEMENTS

We thank Barry Madore, Claudia Maraston, Ian Steer, Richard Stiskalek and Tariq Yasin for useful inputs and discussion. JAN and HD are supported by a Royal Society University Research Fellowship (grant no. 211046).

REFERENCES

- An K., 1933, *Giorn Dell’inst Ital Degli Att*, 4, 89
- Anand G. S., Tully R. B., Rizzi L., Riess A. G., Yuan W., 2022, *The Astrophysical Journal*, 932, 15
- Anderson R. I., 2024, *arXiv e-prints*, p. [arXiv:2403.02801](https://arxiv.org/abs/2403.02801)
- Anton T., Clifton T., 2024, *Journal of Cosmology and Astroparticle Physics*, 2024, 120
- Becker M. R., Desmond H., Rozo E., Marshall P., Rykoff E. S., 2015, *arXiv e-prints*, p. [arXiv:1507.07523](https://arxiv.org/abs/1507.07523)
- Bingham E., et al., 2019, *J. Mach. Learn. Res.*, 20, 28:1
- Boruah S. S., Hudson M. J., Lavaux G., 2020, *Monthly Notices of the Royal Astronomical Society*, 498, 2703
- Bovy J., Hogg D. W., Rix H.-W., 2009, *The Astrophysical Journal*, 704, 1704

- Brout D., et al., 2022, *ApJ*, **938**, 110
- Cappellari M., et al., 2011, *Monthly Notices of the Royal Astronomical Society*, **413**, 813
- Chaparro-Molano G., Cuervo J. C., Restrepo Gaitán O. A., Torres Arzayús S., 2019, *Monthly Notices of the Royal Astronomical Society*, **485**, 4343
- DESI Collaboration et al., 2024, *arXiv e-prints*, p. [arXiv:2404.03002](https://arxiv.org/abs/2404.03002)
- Della Valle M., Livio M., 1994, *Astronomy and Astrophysics*, **286**, 786
- Desmond H., Jain B., Sakstein J., 2019, *Physical Review D*, **100**, 043537
- Desmond H., Sakstein J., Jain B., 2021, *Physical Review D*, **103**, 024028
- Dupuy A., Courtois H. M., 2023, *A&A*, **678**, A176
- Feindt U., et al., 2013, *A&A*, **560**, A90
- Foreman-Mackey D., Hogg D. W., Lang D., Goodman J., 2013, *Publications of the Astronomical Society of the Pacific*, **125**, 306
- Freedman W. L., Madore B. F., 2023, *J. Cosmology Astropart. Phys.*, **2023**, 050
- Freedman W. L., Madore B. F., 2024, in de Grijs R., Whitelock P. A., Catelan M., eds, *IAU Symposium Vol. 376*, *IAU Symposium*. pp 1–14 ([arXiv:2308.02474](https://arxiv.org/abs/2308.02474)), [doi:10.1017/S1743921323003459](https://doi.org/10.1017/S1743921323003459)
- Freedman W. L., et al., 2019b, *The Astrophysical Journal*, **882**, 34
- Freedman W. L., et al., 2019a, *ApJ*, **882**, 34
- Freedman W. L., Madore B. F., Jang I. S., Hoyt T. J., Lee A. J., Owens K. A., 2024, *arXiv e-prints*, p. [arXiv:2408.06153](https://arxiv.org/abs/2408.06153)
- Fusco F., Buonanno R., Bono G., Cassisi S., Monelli M., Pietrinferni A., 2012, *Astronomy & Astrophysics*, **548**, A129
- Hubble E., 1929, *Proceedings of the National Academy of Science*, **15**, 168
- Humphreys E., Greenhill L., Reid M., Argon A., Moran J., 2004, in *American Astronomical Society Meeting Abstracts*. pp 73–01
- Jang I. S., et al., 2022, TRGB and Cepheid distance scales: is there local tension?, HST Proposal. Cycle 30, ID. #17079
- Karachentsev I. D., Makarov D. I., Kaisina E. I., 2013, *The Astronomical Journal*, **145**, 101
- Kullback S., Leibler R. A., 1951, *The annals of mathematical statistics*, **22**, 79
- Kushnir D., Sharon A., 2024, *arXiv preprint arXiv:2404.16102*
- Lee M. G., Freedman W. L., Madore B. F., 1993, *ApJ*, **417**, 553
- Lee A. J., Freedman W. L., Madore B. F., Jang I. S., Owens K. A., Hoyt T. J., 2024, *arXiv e-prints*, p. [arXiv:2408.03474](https://arxiv.org/abs/2408.03474)
- Lépine S., Koch A., Rich R. M., Kuijken K., 2011, *The Astrophysical Journal*, **741**, 100
- Li S., Beaton R. L., 2024, *arXiv e-prints*, p. [arXiv:2403.17048](https://arxiv.org/abs/2403.17048)
- Li X., Keeley R. E., Shafieloo A., Zheng X., Cao S., Biesiada M., Zhu Z.-H., 2021, *Monthly Notices of the Royal Astronomical Society*, **507**, 919
- Lyall S., Blake C., Turner R., Ruggeri R., Winther H., 2023, *Monthly Notices of the Royal Astronomical Society*, **518**, 5929
- Lyall S., Blake C., Turner R. J., 2024, *Monthly Notices of the Royal Astronomical Society*, **532**, 3972
- MacKay D. J., 2003, *Information theory, inference and learning algorithms*. Cambridge university press
- Madore B. F., Freedman W. L., 2020, *ApJ*, **899**, 66
- Madore B., Freedman W., 2024a, in *American Astronomical Society Meeting Abstracts*. p. 418.03
- Madore B. F., Freedman W. L., 2024b, *ApJ*, **961**, 166
- Mai-Jalanobis P., 1936, in *Proc. Nat. Inst. India*. pp 44–55
- McMillan P. J., 2016, *Monthly Notices of the Royal Astronomical Society*, p. stw2759
- Ohlson D., Seth A. C., Gallo E., Baldassare V. F., Greene J. E., 2023, *The Astronomical Journal*, **167**, 31
- Owens K. A., Madore B. F., Freedman W. L., 2021, *Understanding Systematic Errors in the Cepheid Distance Scale*, HST Proposal. Cycle 29, ID. #16627
- Owens K. A., Freedman W. L., Madore B. F., Lee A. J., 2022, *ApJ*, **927**, 8
- Owens K., Jang I. S., Freedman W., Hoyt T., Lee A., Madore B., Monson A., 2024, in *American Astronomical Society Meeting Abstracts*. p. 441.05
- Perlmutter S., et al., 1999, *ApJ*, **517**, 565
- Phan D., Pradhan N., Jankowiak M., 2019, *arXiv preprint arXiv:1912.11554*
- Pourojaghi S., Zabihi N., Malekjani M., 2022, *Physical Review D*, **106**, 123523
- Reid M., Pesce D. W., Riess A., 2019, *The Astrophysical Journal Letters*, **886**, L27
- Rezaei M., Solà Peracaula J., Malekjani M., 2022, *Monthly Notices of the Royal Astronomical Society*, **509**, 2593
- Rich J. A., Persson S., Freedman W. L., Madore B. F., Monson A. J., Scowcroft V., Seibert M., 2014, *The Astrophysical Journal*, **794**, 107
- Riess A. G., Breuval L., 2024, in de Grijs R., Whitelock P. A., Catelan M., eds, *IAU Symposium Vol. 376*, *IAU Symposium*. pp 15–29 ([arXiv:2308.10954](https://arxiv.org/abs/2308.10954)), [doi:10.1017/S1743921323003034](https://doi.org/10.1017/S1743921323003034)
- Riess A. G., et al., 1998, *AJ*, **116**, 1009
- Riess A. G., et al., 2009, *The Astrophysical Journal*, **699**, 539
- Riess A. G., et al., 2011, *The Astrophysical Journal*, **730**, 119
- Riess A. G., Fliri J., Valls-Gabaud D., 2012, *The Astrophysical Journal*, **745**, 156
- Riess A. G., et al., 2022, *The Astrophysical journal letters*, **934**, L7
- Riess A. G., et al., 2024a, *The Astrophysical Journal Letters*, **962**, L17
- Riess A. G., et al., 2024b, *The Astrophysical Journal*, **977**, 120
- Rigault M., et al., 2015, *The Astrophysical Journal*, **802**, 20
- Rigault M., et al., 2020, *Astronomy & Astrophysics*, **644**, A176
- Rubin D., et al., 2023, *arXiv e-prints*, p. [arXiv:2311.12098](https://arxiv.org/abs/2311.12098)
- Said K., Colless M., Magoulas C., Lucey J. R., Hudson M. J., 2020, *Monthly Notices of the Royal Astronomical Society*, **497**, 1275
- Sbarufatti B., Treves A., Falomo R., 2005, *The Astrophysical Journal*, **635**, 173
- Schmidt-Kaler T., Oestreicher M., 1998, *Astronomische Nachrichten*, **319**, 375
- Scolnic D., et al., 2023, *The Astrophysical Journal Letters*, **954**, L31
- Scott D. W., 2015, *Multivariate density estimation: theory, practice, and visualization*. John Wiley & Sons
- Silverman B. W., 2018, *Density estimation for statistics and data analysis*. Routledge
- Singh R., 2021, *Ap&SS*, **366**, 99
- Smirnov N., 1948, *The annals of mathematical statistics*, **19**, 279
- Steer I., 2020, *AJ*, **160**, 199
- Steer I., et al., 2016, *The Astronomical Journal*, **153**, 37
- Stiskalek R., Desmond H., Devriendt J., Slyz A., Lavaux G., Hudson M. J., Bartlett D. J., Courtois H. M., 2025, *arXiv e-prints*, p. [arXiv:2502.00121](https://arxiv.org/abs/2502.00121)
- Strader J., Smith G. H., Larsen S., Brodie J. P., Huchra J. P., 2009, *The Astronomical Journal*, **138**, 547
- Strauss M. A., Willick J. A., 1995, *Phys. Rep.*, **261**, 271
- Turner R. J., 2024, *arXiv e-prints*, p. [arXiv:2411.19484](https://arxiv.org/abs/2411.19484)
- Uddin S. A., et al., 2024, *The Astrophysical Journal*, **970**, 72
- Valade A., Libeskind N. I., Pomarède D., Tully R. B., Hoffman Y., Pfeifer S., Kourkchi E., 2024, *Nature Astronomy*, **8**, 1610
- Vincenzi M., et al., 2024, *ApJ*, **975**, 86
- Virtanen P., et al., 2020, *Nature methods*, **17**, 261
- Walborn N. R., Blades J. C., 1997, *The Astrophysical Journal Supplement Series*, **112**, 457
- Watkins R., et al., 2023, *MNRAS*, **524**, 1885
- Zaninetti L., 2023, *Journal of High Energy Physics, Gravitation and Cosmology*, **10**, 8

Table 1. As Table 1 but including only measurements that can be standardised through either H_0 or μ_{LMC} .

Distance indicator	# of galaxies	# pairs	# total measurements/references	KL p -value	External consistency
CMD	20	3454	1265 / 170	0.9812	11 / 20
BL Lac Luminosity	2	2	20 / 11	0.9215	-
RR Lyrae	8	38	26409 / 216	0.8031	13 / 26
TRGB	2	2	1736 / 336	0.4473	5 / 18
RV Stars	1	10	5 / 1	0.087	-
Cepheids	36	1157	10956 / 325	0.0	2 / 39
GRB	86	1214	729 / 17	0.0	-
SNIa SDSS	1849	7687	6054 / 1	0.0	0 / 2
Type II Cepheids	2	13	62 / 22	0.0	10 / 18
SNIa	4856	117978	30843 / 140	0.0	7 / 25
AGN time lag	0	0	32 / 3	-	2 / 3
AGB	0	0	2 / 2	-	1 / 2
B Stars	0	0	2 / 2	-	2 / 3
Black Hole	0	0	17 / 2	-	2 / 2
Blue Supergiant	0	0	2 / 1	-	3 / 5
BCG	0	0	239 / 1	-	2 / 3
Brightest Stars	0	0	129 / 41	-	0 / 6
Carbon Stars	0	0	82 / 13	-	12 / 16
Delta Scuti	0	0	12 / 2	-	4 / 7
FGLR	0	0	7 / 7	-	0 / 3
GCLF	0	0	781 / 96	-	5 / 16
GC SBF	0	0	3 / 1	-	6 / 9
HII LF	0	0	17 / 2	-	0 / 4
Horizontal Branch	0	0	110 / 53	-	5 / 11
M Stars	0	0	6 / 5	-	2 / 6
Miras	0	0	36 / 27	-	8 / 15
Novae	0	0	18 / 11	-	11 / 17
OB Stars	0	0	4 / 3	-	6 / 7
PNLF	0	0	183 / 57	-	2 / 6
Red Clump	0	0	236 / 63	-	8 / 14
RSV Stars	0	0	9 / 6	-	3 / 8
SX Phe Stars	0	0	3 / 2	-	0 / 1
Statistical	0	0	292 / 27	-	14 / 37
Subdwarf fitting	0	0	1 / 1	-	0 / 1
SZ effect	0	0	283 / 19	-	4 / 5
SBF	0	0	1781 / 67	-	2 / 14
SNIi radio	0	0	24 / 2	-	2 / 6
White Dwarfs	0	0	1 / 1	-	0 / 1
Grav. Wave	0	0	8 / 8	-	1 / 1

APPENDIX A: RESULTS WITH STANDARDISABLE MEASUREMENTS ONLY

Here we show the analogues of Tables 1 and 2 but excluding measurements that do not list a H_0 or μ_{LMC} value and hence cannot be standardised. On the whole we find that the consistency little improves, indicating that the non-standardisability of many of the measurements was not a principal cause of inconsistency in the main text. For this reason we do not show the results after rescaling the uncertainties and/or shifting the means. We do however find that behaviour of the CMD indicator improves dramatically. This method also has a significant number of measurements, suggesting that it may be useful for constraining the distance ladder.

Table A1. As Table 2 but including only measurements that can be standardised through either H_0 or μ_{LMC} .

Distance indicator	# of galaxies	# pairs	# total measurements/references	KL p -value	External consistency
SNII optical	128	390	1622 / 89	0.0	1 / 7
Dwarf Galaxy Diameter	0	0	16 / 1	-	6 / 9
Eclipsing Binary	0	0	273 / 48	-	9 / 15
GC radius	0	0	101 / 8	-	1 / 11
G Lens	0	0	86 / 14	-	0 / 1
HII region diameter	0	0	53 / 7	-	1 / 12
Maser	0	0	24 / 20	-	4 / 8
Orbital Mech.	0	0	3 / 3	-	0 / 2
Proper Motion	0	0	5 / 3	-	2 / 3
Ring Diameter	0	0	212 / 1	-	2 / 4
GeV TeV ratio	3	5	30 / 11	0.0124	-
Faber-Jackson	427	1907	1424 / 6	0.0016	4 / 18
D-Sigma	548	2787	1995 / 9	0.0	9 / 16
FP	807	1134	130214 / 22	0.0	7 / 22
IRAS	404	639	2947 / 2	0.0	3 / 28
Tully-Fisher	4972	99919	56436 / 78	0.0	11 / 44
Diameter	0	0	6 / 2	-	9 / 15
GC FP	0	0	3 / 3	-	7 / 9
H I + optical distribution	0	0	1 / 1	-	0 / 1
LSB galaxies	0	0	2 / 1	-	1 / 4
Magnitude	0	0	111 / 3	-	1 / 9
Sosies	0	0	287 / 3	-	1 / 4
Tertiary	0	0	284 / 4	-	5 / 12
Tully est	0	0	1434 / 1	-	17 / 27